

# Evaluation of Experimental Laser-Induced-Damage Assessment Techniques For Solid-State Nonlinear Optical Elements

Brian R. Kimball\*

Materials Science Team, U.S. Army Soldier Systems Center, Natick, MA 01760

Kenneth Altshuler

Physics Department, Wayland High School, Wayland, MA 01778

Samuel Cohen, Barry DeCristofano, Masato Nakashima

Materials Science Team, U.S. Army Soldier Systems Center, Natick, MA 01760

Appaji Panchangam, D.V.G.L.N. Rao, Pengfei Wu

University of Massachusetts-Boston, Physics Department, Boston MA 02125,

## ABSTRACT

A comparison is made of two, laser-induced-damage assessment techniques. The first technique monitors the sample for changes in linear transmission after high-energy laser illumination. With the second technique, an image is transmitted through the sample, after high-energy laser illumination, at the position of incidence. Both single and multiple shot data are considered. Results show the imaging technique to be an efficient method by which to unambiguously discern the onset of image-degrading laser-damage, regardless of detector noise, shot-to-shot variations and sample inhomogeneities. Practically speaking, the imaging technique is relatively easy to incorporate into a laser-based experimental system and is particularly relevant to the assessment of optical systems for imaging.

**KEY WORDS:** Laser-induced damage, nonlinear optics, damage threshold, nonlinear absorption, nanosecond laser pulses, single shot, multiple shot, linear transmission

## 1. INTRODUCTION

It is often necessary to create large flux densities within a nonlinear optical element in order to trigger a desired NLO event. This is often done by focusing the energy source (laser) into the system and monitoring the throughput for the information of interest. With such high flux densities, there is a danger of damage to the element. A common technique for monitoring the sample for damage is to monitor changes in transmission that are not associated with a desired NLO effect. In some cases the damage can be catastrophic. For example, there may be surface damage or localized stress cracks that become immediately apparent when monitoring transmission. The possibility exists, however, that more subtle changes can be occurring at the surface or within the bulk of the element at lower incident fluences that are not apparent through changes in transmission, but yet may significantly degrade the performance. The aim of this study is to examine the effectiveness of the transmission method for damage assessment by utilizing another technique that can be used to detect damage. With the latter technique, an image is transmitted through the optical element at the possible damage site. The resolution of the image is then monitored for changes that are a consequence of laser-induced damage.

### 1.1 Bulk Effects

Dielectric breakdown can be induced in bulk materials by high power laser radiation. Typical AC dielectric breakdown strengths vary from about 1 to 5 MV cm<sup>-1</sup>. Respective power densities range from 50 to 1000 MW mm<sup>-2</sup>. In general, breakdown strength is independent of wavelength except through the refractive index and focused spot size<sup>1</sup>. Measured



laser induced damage thresholds (LIDT) tend to be much lower than calculated values, sometimes by as much as two orders of magnitude. This is due to absorption, which can be influenced by surface conditions such as cracks, grooves, scratches, pores or absorptive inclusions. Whereas such conditions tend, by nature, to be random, a given sample can show a fairly wide range of LIDTs from one location to the next.

### 1.2 Surface Effects

Surface damage generally occurs before dielectric breakdown in optical systems employing lasers. Experimentally determined damage thresholds in air appear to be higher for the front surface than for the back surface. Interestingly, once surface reflections and phase shifts are accounted for, breakdown intensities are equal for front and back surfaces<sup>1</sup>. When laser light is incident on a surface, the reflected and incident wave generate maximum constructive power density a distance  $\lambda/2$  from the surface. This can result in the formation of plasma in the air in the case of a front surface. The absorption of energy required to produce the plasma can actually help protect the surface. It is not unusual to observe plasma formation, in the form of bright sparks, at power densities below the onset of damage. At the rear surface, however, the standing wave and associated maximum constructive power density occurs within the bulk material, thus causing formation of plasma within the material, resulting in catastrophic damage<sup>2,3</sup>.

Surface imperfections tend to create reflections, diffraction or lensing, all of which can cause constructive interference within the sample and lead to damage thresholds sometimes up to a factor of 100 times below the intrinsic value. By careful polishing and cleaning of a surface, where scratches are reduced to less than one hundredth of the incident wavelength, one can realize experimental damage thresholds on the same order of magnitude as the intrinsic bulk damage threshold. Using theoretical considerations, Bloembergen<sup>4</sup> has derived expressions for electric field ( $V$ ) enhancement due to scratches, grooves and pores:

$$\text{Scratch:} \quad V = n^2 V_o \quad (1)$$

$$\text{Groove:} \quad V = \frac{2n^2}{(n^2 + 1)} V_o \quad (2)$$

$$\text{Pore:} \quad V = \frac{3n^2}{2n^2 + 1} V_o \quad (3)$$

where  $V_o$  is the incident electric field and  $n$  is the index of refraction of the medium. The electric field enhancement is linear with incident field for all three cases. For  $n=1.5$  the enhancement is 125% for a scratch, 38% for a groove and 23% for a pore.

## 2. EXPERIMENTAL SETUP

An  $f/5$  focusing geometry was used to evaluate laser-induced damage. A schematic is shown in Fig.1. A frequency doubled Nd:YAG laser was used to create 10 ns pulses at 10 Hz repetition rate. The diameter of the beam at the laser output is approximately 1 cm. Residual 1064 nm radiation is removed from the beam by a filter located at the laser output. Filters at ND-1 are used to control the energy entering the measurement system. A beam splitter directs approximately 10% of the incident energy toward detector-A, which is used to monitor and compensate for variations in laser output. Filters at ND-2 are used to balance energy within the system. The beam passes through a 6.67 mm diameter aperture and is then incident on a negative 1951 USAF resolution target measuring 2x2 inches. A 33 mm focal length lens then focuses the laser energy into the sample under study. A 70 mm lens collects light emerging from the sample and focuses the resolution target image onto a CCD array. A beam splitter directs a portion of the transmitted energy to detector C, which is used to monitor changes in transmission. Neutral density filters at ND-3 are used to balance the dynamic range of the system. Data were acquired via PC-based, commercial data acquisition and analysis software. A LeCroy LC574A 1 GHz digital oscilloscope was used for some portions of the study.

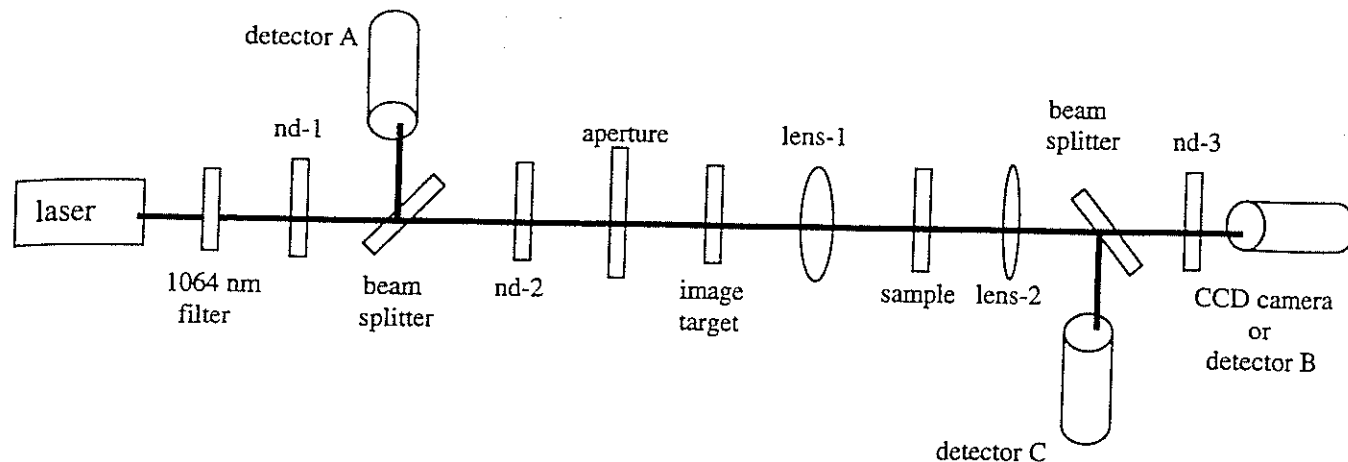


Figure 1. Experimental Setup

Throughout this study, a single solid polyurethane sample was used. The sample is approximately 2 mm thick and measures 2 X 2 inches. The sample was located at the focus of lens 1 shown in Fig. 1. The measured focused spot diameter was 40 $\mu$ m. The sample was tested for evidence of nonlinear absorption, but no such effect was found. Damage induced changes in transmission were monitored for each laser pulse by taking the ratio of voltage readings at detectors C and A:

$$T = \frac{V_{Det - C}}{V_{Det - A}} \quad (4)$$

This also compensates for variations in laser output. For each laser pulse incident on the sample, an image of the 1951 USAF resolution target was recorded with a CCD camera. For each experimental run an appropriate set of lines and spaces was chosen, based on target resolution and number of pixels, and used throughout the run. Image degradation was noted visually and quantified by calculating the modulation of a line scan through the image.

$$modulation = \frac{(I_{max} - I_{min})}{(I_{max} + I_{min})} \quad (5)$$

The highest pixel intensity at each of the three lines is determined for the line-space set under study.  $I_{max}$  is taken as the median of the three values.  $I_{min}$  is the average of the highest pixel intensity for the two corresponding spaces in the set. The modulation is calculated for each image relating to each pulse and plotted as a function of input energy or pulse count.

### 3. SINGLE SHOT VERSUS MULTIPLE SHOT DAMAGE ASSESSMENT

Here, two general cases are considered: single and multiple shot. For the single shot case, damage occurs within, or shortly after the duration of the pulse, depending on the pulse length and temporal profile. For the multiple shot case, damage may be the result of cumulative effects occurring during the course of the pulse train.

#### 3.1 Single Shot Analysis

For the single shot case, the effort to determine the onset of laser-induced damage involves the recording of single laser pulses, with each shot incident on a new location of the sample. In this way cumulative effects are avoided. A number of single shot runs were performed for this study in order to investigate various aspects of laser-induced damage.

Case 1: It is possible that nonlinear effects could reversibly alter both the transmission and modulation recorded at the throughput detector or CCD camera. For example, thermal lensing can defocus the beam and distort the image during the period that the pulse is incident on the sample. Also, under certain conditions damage may not occur until the latter part of a laser pulse and consequently can go undetected by the measurement system. With this in mind, a single shot run was performed where three pulses were recorded at each location on the sample. The three shots consist of a low-energy, high-energy, low-energy scheme. At each successive location on the sample the energy of the high-energy pulse is increased while the energy of the low-energy pulse stays the same throughout the experimental run. Low energy-pulse levels are kept below the damage threshold and the level at which there are detectable nonlinear effects. The first pulse represents the standard against which the following two are compared. The second, high-energy pulse creates the damage and the final, low-energy pulse checks for damage. The transmission is calculated for both low-energy pulses using Eq.4 and then normalized. The two transmission values are then compared:

$$T_{normal} = \frac{(T_{pulse - 3})}{(T_{pulse - 1})} \quad (6)$$

This compensates for pulse-to-pulse variations in laser output as well as variations in the localized transmission of the sample. It does not, however, eliminate digitization noise or various types of electrical noise associated with the energy measurement system, which are evident in the plots. The results of Eq. 6 are then plotted as a function of input energy for the entire run.

Using the CCD camera, an image was acquired for all three pulses within a set. Visual comparisons were made of all three images and the modulation was calculated for each using Eq. 5. Transmission values were calculated using Eq. 6. The results are shown in Fig. 2.

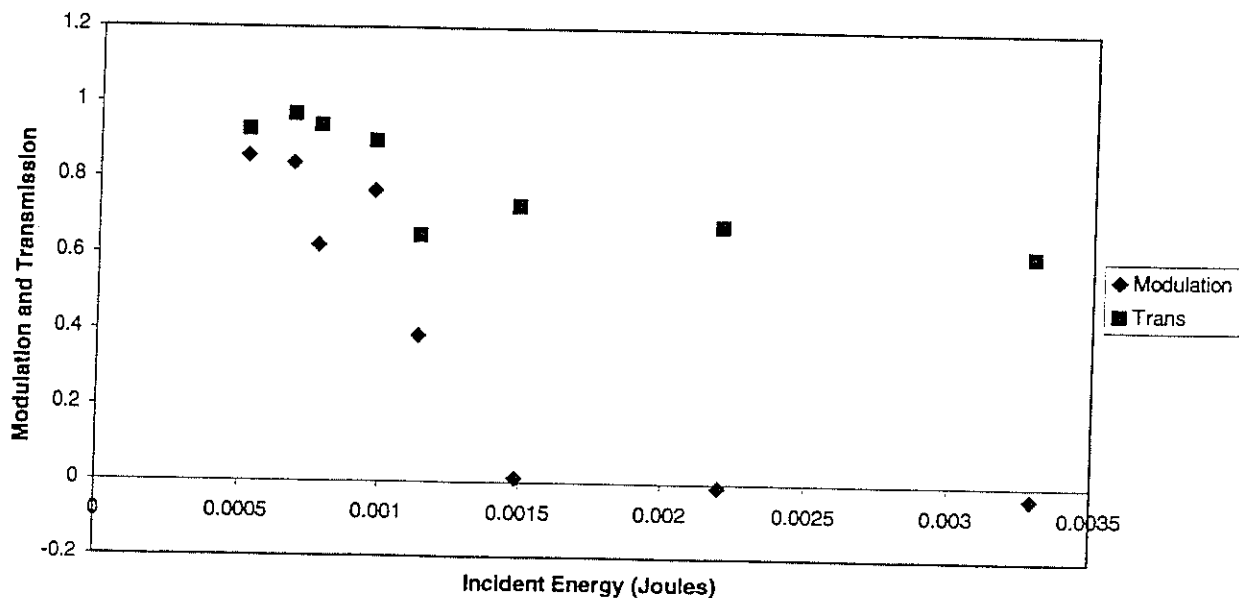


Figure 2. Modulation and transmission versus input energy for single-shot data.

The transmission curve shown in Fig. 2 falls off more slowly than the modulation. This may be more an artifact of the particular experimental setup used in the study than an indication that the modulation method is more sensitive. Transmission sensitivity can be increased by placing an aperture before the throughput detector to reduce scattered light from the damage site into the detector. The modulation curve in Fig. 2 shows some variation in the point at which it begins to fall off from the linear region. Close study of the data indicates that the variations are real and are attributed to local variations in sample characteristics such as surface condition and inclusions. Variations in modulation values were attributed, in some cases, to shot-to-shot variations in the laser beam spatial profile. Visual inspection via line scans was found to be the most reliable method of ascertaining the onset of laser induced damage. Image blur in the spaces of the resolution chart image becomes immediately apparent to the observer.

Using a silicon photodiode and a 1 GHz digital oscilloscope a trace was generated of the temporal profile of the laser used in the analysis. This trace was compared to that of a single shot pulse creating damage to the sample. The traces are shown in Fig. 3. Deviation is evident between the two traces early on in the pulse indicating the early onset of damage for this energy level and experimental configuration.

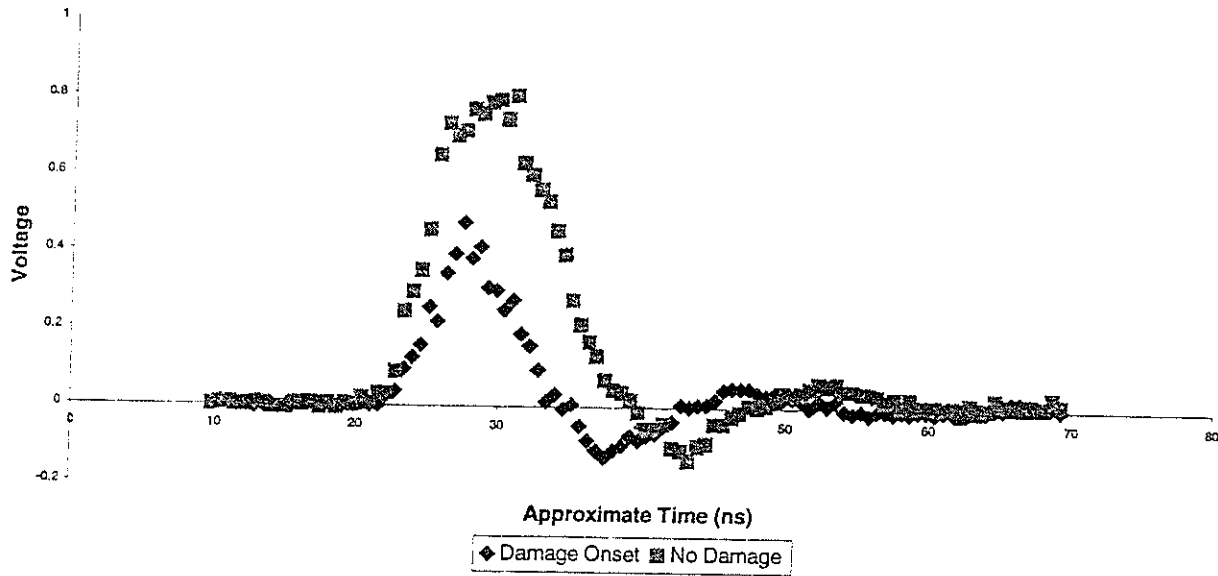


Figure 3. Oscilloscope traces showing laser spatial profile before damage and during damage onset.

Case 2: To reduce noise and thus improve reliability in the assessment of single shot transmission and modulation values, another single-shot run was performed. In this study a number of single shot pulses were recorded for a given input energy, each at a different sample location. Transmission and modulation values were calculated for each pulse. Data relating to a specific energy level were then averaged. The results are shown in Fig.4.

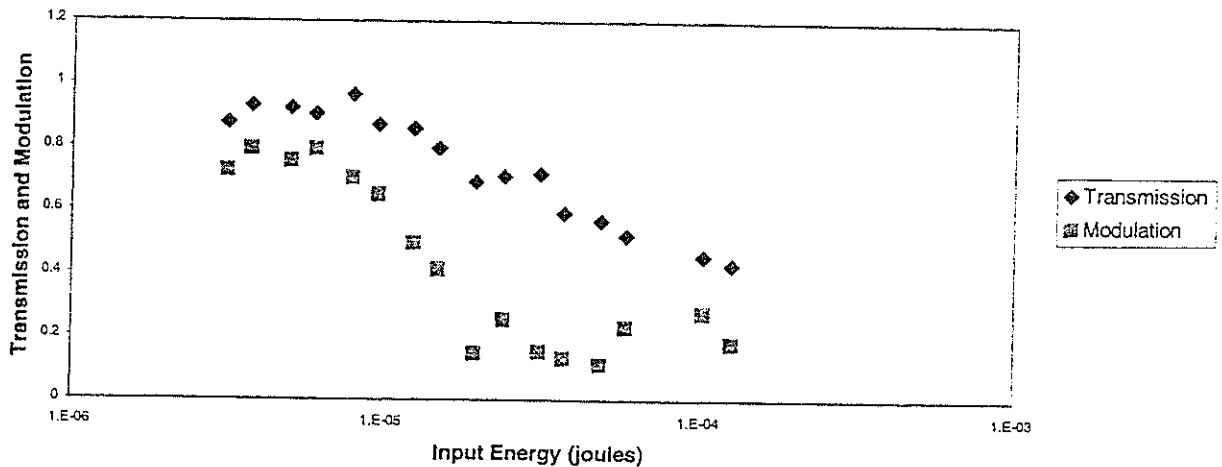


Figure 4. Transmission and modulation versus input energy for averaged single-shot data.

As with the results shown in Fig. 2 for Case 1, the modulation deviates from the linear region at a lower energy than the transmission curve, indicating a higher sensitivity as a damage assessment tool. Noise in the linear region makes it difficult to determine the point at which damage occurs for both the modulation and the transmission curves. The noise is due in part to differences in the damage threshold from one location to the next. Without actually seeing the potential damage site, it is difficult to know whether small changes are due to damage or noise. However, in the modulation case, visual inspection of the image allows one to detect the onset of damage-induced image blur regardless of the noise source. One might conclude from the transmission curve that damage had occurred at point 9. By visual inspection of the images we conclude that damage actually occurred at point 5.

### 3.2 Multiple Shot Analysis

The imaging software used in the study was capable of acquiring images in groups of eight. In order to observe damage phenomena beyond the eight-image limitation, images were acquired in successive groups of eight. That is, images relating to the first eight incident pulses at one sample location were acquired, then images relating to pulses 9 – 16 were recorded at a new sample location etc. This process was repeated until an adequate series of images was acquired depicting various aspects of laser-induced damage.

For the multiple shot data, the laser energy level was set such that cumulative damage would occur between the 5<sup>th</sup> and 10<sup>th</sup> pulse thereby establishing a pre-damage region of linear transmission to which subsequent post-damage data could be compared.

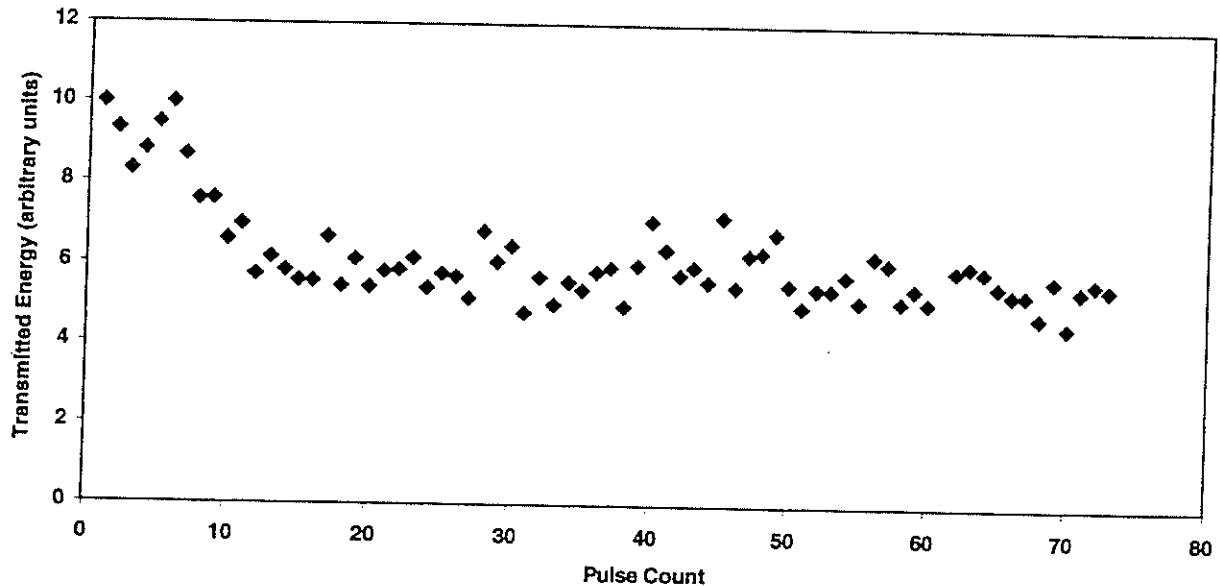


Figure 5. Transmitted energy versus pulse count for multiple shot data.

Figure 5 shows transmitted energy as a function of pulse count for a damaged sample. The decrease in throughput energy is attributed to increased scattering at the damage site. The change in transmission is system-specific in that it can be altered by varying the location of the CCD camera, or the size and location of an aperture located after the sample and before the throughput detector.

The general trend shown in Fig. 5 is repeated in terms of image degradation in Fig. 6. Here modulation is calculated using Eq. 5 for two different runs where data were acquired as described above. Again, the linear region is evident for about the first 10 pulses after which a clear change in modulation can be seen. Discontinuities in the data are due to the images being acquired in groups of eight. This variation is of interest because it shows the way in which the damage threshold of a material can change from one location to another due to variations in surface characteristics, inclusions and subtle changes in the intrinsic polymer mechanical properties.

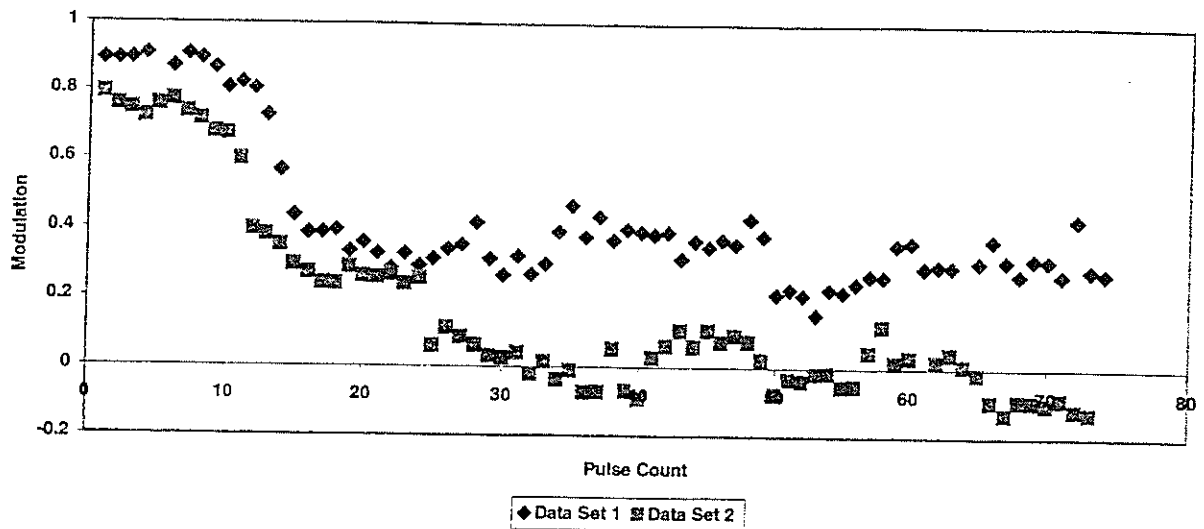


Figure 6. Modulation versus pulse count for two sets of multiple shot data.

This variation in damage threshold was particularly evident in one multiple shot run. In the data set shown in Fig. 7, there is variation of about ten pulses between the 3<sup>rd</sup> and 4<sup>th</sup> groups-of-eight where the modulation goes to zero. The sample location where the 4<sup>th</sup> set of eight images was acquired appears to be particularly robust.

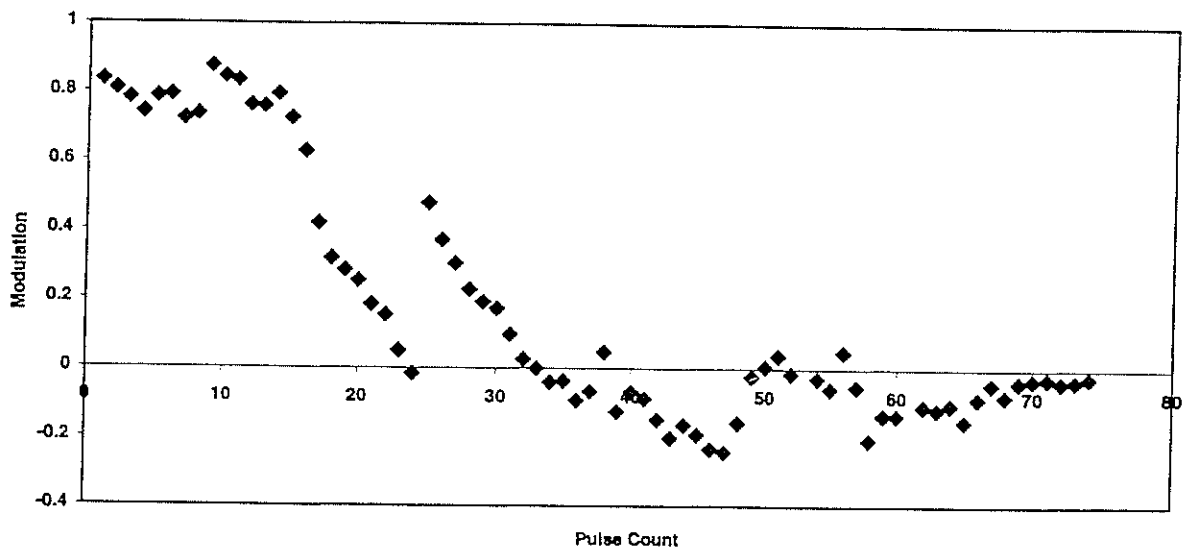


Figure 7. Modulation versus pulse count for multiple-shot data. Data depicts variation in localized damage threshold for a single sample.

Figure 8 shows three images depicting various stages of damage during a multiple shot run similar to that shown in Fig. 7. In the first image, the line scans show well defined contrast between the lines and spaces of the resolution pattern. The spaces of the second image show increased image blur associated with the damage site. In the third image the pattern is barely discernable. It is by observing the point at which the spaces begin to show intensity growth that one is able to determine the onset of laser-induced damage.

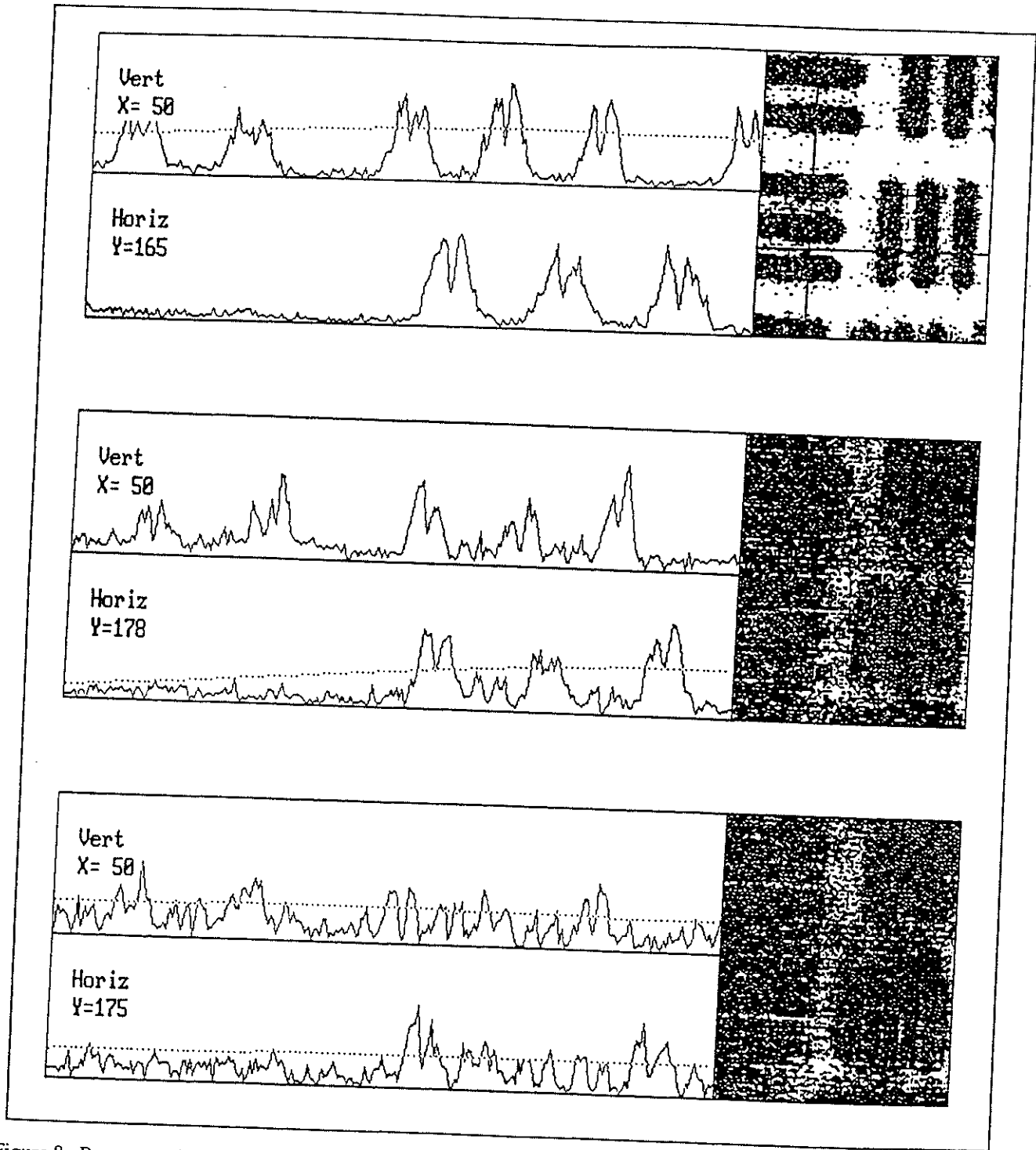
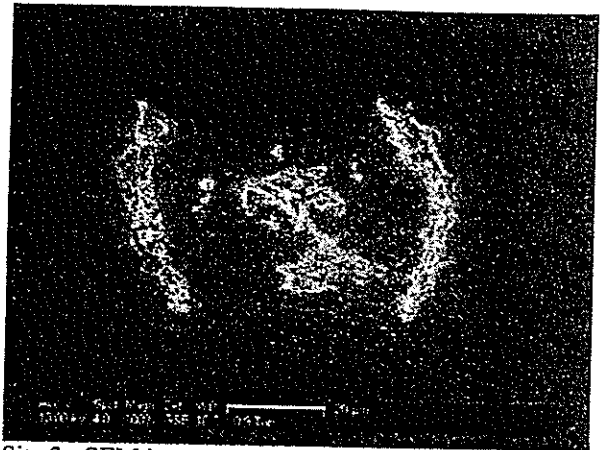


Figure 8. Representative images and corresponding line scans for three data points used to calculate image modulation

Figure 9 shows micrographs of representative damage sites. These do not correlate with the images shown in Figure 8. Sample transmission before damage was near 100%. Transmission through damage sites 2, 3 & 4 was 1.3%, 8.4% and 14%, respectively. SEM images were acquired using a Philips XL30 Electroscan. Light microscope images were obtained via a Zeiss Ultraphot.



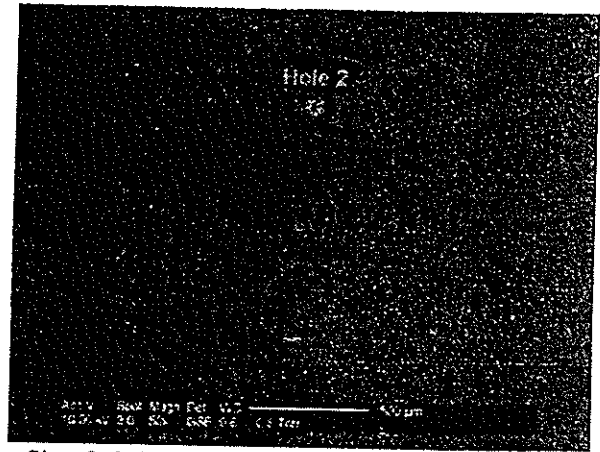
Site 2: SEM image, 1000x, incident energy = 2.1 mJ



Site 3: SEM image, 1000x, incident energy = 1.2 mJ



Site 4: SEM image, 1000x, incident energy = 0.7 mJ



Sites 2, 3 & 4: Light microscope image, 50x

Figure 9. SEM micrographs of laser damage sites. Hole 2 is designated on the sample micrograph, followed by holes 3 and 4.

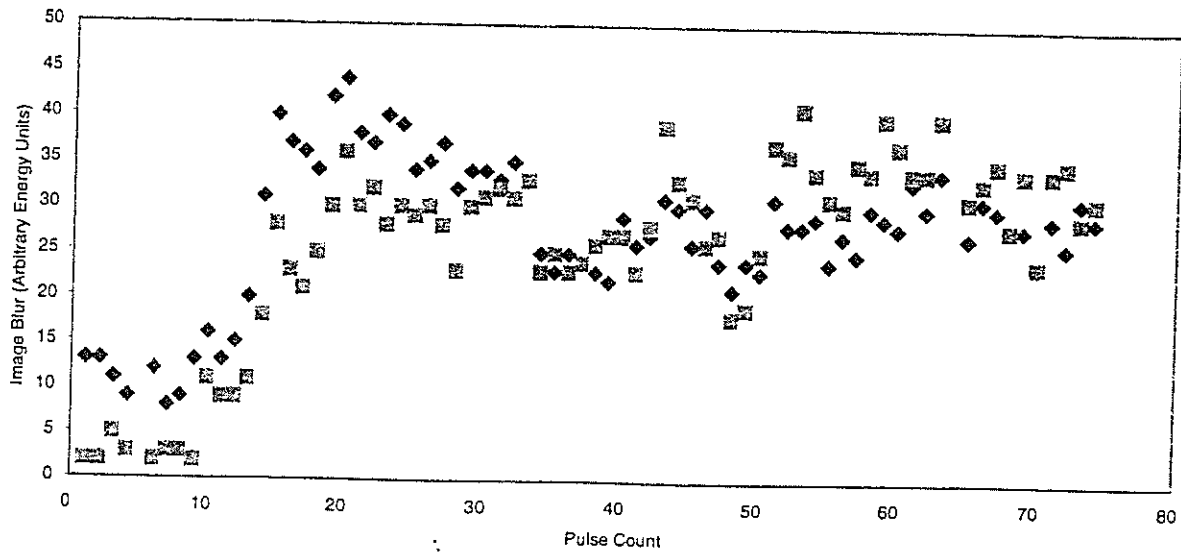


Fig. 10. Image blur intensity versus pulse count for multiple shot data.

In Fig. 10 the pixel intensity of the spaces in the line/space groups is plotted versus pulse count for two sets of data. A general trend is evident: as the sample becomes increasingly more damaged, the energy is displaced from the lines to the spaces of the image. In Fig. 11 a comparison is shown between modulation for a single-shot run and a multiple-shot run. Energy is cumulative for the multiple shot-data. That is, energy plotted for a given shot is actually a summation of energies from all previous shots to that of it's own. The multiple-shot data shows a higher damage threshold than the single-shot owing to the dissipation of energy as heat between pulses.

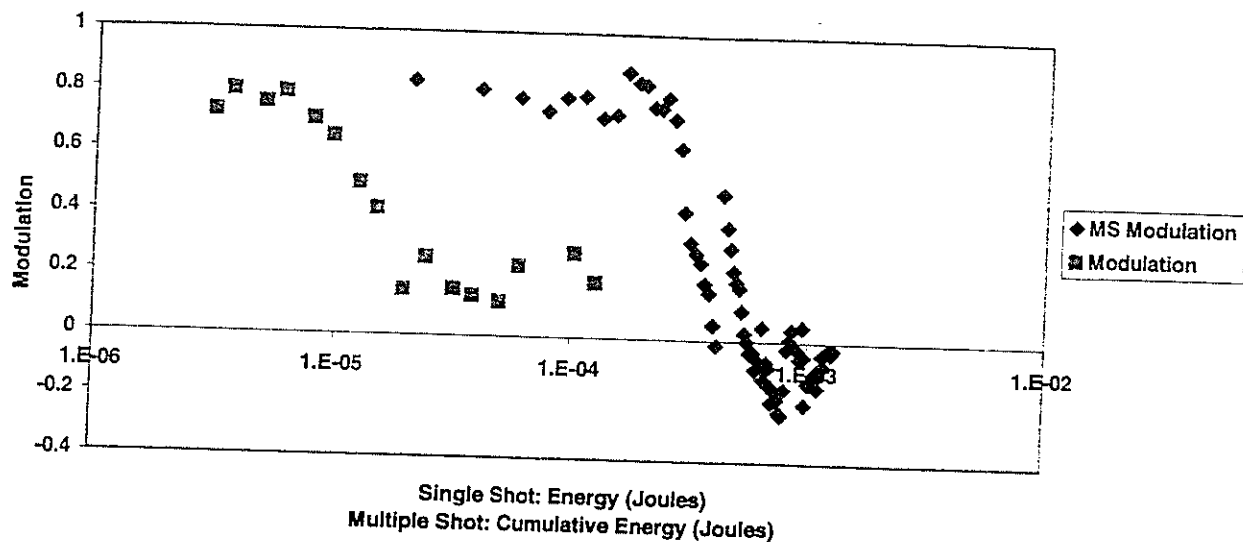


Fig. 11. Single-shot and multiple-shot modulation versus input energy.

## CONCLUSION

Two laser-induced-damage assessment techniques were evaluated and compared for applicability to optical systems used for imaging. In general, modulation values appeared to be a more sensitive damage assessment indicator than transmission values. This can be attributed to a larger range of possible modulation values, which can be from 1 to a number less than zero, as was the case in this study. For samples that show absorption at the incident wavelength, the difference in sensitivity between the two techniques is expected to be greater, because of the reduction in the range of possible transmission values.

Though this study indicates that modulation is a more sensitive measure of the onset of laser-induced damage, the technique is still susceptible to experimental variations, especially shot-to-shot variations in laser output power and beam spatial profile, both of which cause variations in the dynamic range of the measurement system. In a quantitative sense then, the issue of determining the point at which damage occurs is still present in both techniques. Qualitatively, however, a relatively more reliable assessment technique is by visual inspection of the data via a line scan through the image. Through visual inspection it is possible to discern whether decreased modulation or transmission is due to system noise, or to actual image degradation associated with damage at the site.

## REFERENCES

1. R. M. Wood, *Laser Damage in Optical Materials*, Arrowsmith Ltd, Bristol, 1986.
2. N. L. Boling, M. D. Crisp and G. Dube, "Laser Induced Surface Damage," *Appl. Opt.* 12, No. 4, pp. 650-660, 1973.
3. A. J. Glass and A. H. Guenther, "Laser Induced Damage of Optical Elements - a Status Report," *Appl. Opt.* 12, No. 4, pp. 637-649, 1973.
4. N. Bloembergen, "Role of Cracks, Pores, and Absorbing Inclusions on Laser Induced Damage Threshold at Surfaces of Transparent Dielectrics," *Appl. Opt.* 12, 661-664, 1973.